

Supplement to “Pervasive diffusion of climate signals recorded in ice-vein ionic impurities”

by Felix S. L. Ng

- 5 Movies S1–S8: Here, captions only. Access the movies via doi:10.15131/shef.data.12739169.
Please use <https://figshare.com/s/aa059ab52b73f472f3fd> during the review stage.

Figs. S1–S3

- 10 **Movie S1:** Modelled evolution of a signal peak in our GRIP control run (top panels) and an otherwise identical run where the Gibbs–Thomson effect is turned off by setting $\gamma = 0$ (bottom panels), from 0.5 to 130 kyr. The horizontal coordinate z' measures displacement in the material reference frame. Near the top left, t denotes the age of the ice at $z' = 0$, and z its depth below the surface; t and z apply to the movie frames in both runs. The simulated variables are bulk solute concentration c_B (left), vein solute concentration c (middle), anomalous velocity w_c , porosity ϕ and vein curvature r_v (right). Grey curves in the left-hand
15 panels indicate the initial doped peak. Snapshots from the movie are shown in Fig. 5.

Movie S2: Modelled evolution of a signal peak in our EPICA control run (top panels) and an otherwise identical run where the Gibbs–Thomson effect is turned off by setting $\gamma = 0$ (bottom panels), from 4 to 460 kyr. The panels are as organised in Movie S1. Snapshots from the movie are shown in Fig. 6.

- 20 **Movie S3:** Modelled evolution of two neighbouring peaks in a GRIP run from 0.5 to 70 kyr, using the control parameters of the run in Fig. 5a and Movie S1 (top panels). t denotes the age of the ice at $z' = 0$, and z its depth below the surface. Diffusional spreading causes the peaks to merge as they approach each other under vertical compression. Snapshots from the movie are shown in Fig. 10.

- 25 **Movie S4:** Simulated evolution of a 20-m long sequence of c_B signals at the GRIP site from 0.5 to 100 kyr, in three experiments assuming the molecular diffusivities D (Table 1), $0.1D$ and $0.03D$. t denotes the age of the ice at $z' = 0$, and z its depth below the surface. The initial doped signal is made from the superposition of 300 random Gaussian peaks at decimetre scale. The upper panel shows the whole signal sequence as it evolves, resizing the axes occasionally to expand upon details. The lower panel focusses on the stretch $z' = -2$ to 2 m.

Movie S5: Simulated evolution of a 80-m long sequence of c_B signals at the EPICA site from 5 to 500 kyr, in three experiments
30 assuming the molecular diffusivities D (Table 1), $0.1D$ and $0.03D$. t denotes the age of the ice at $z' = 0$, and z its depth below
the surface. The initial doped signal is made from the superposition of 1200 random Gaussian peaks at decimetre scale. The
upper panel shows the whole signal sequence as it evolves, resizing the axes occasionally to expand upon details. The lower
panel focusses on the stretch $z' = -5$ to 5 m. Snapshots from the movie are shown in Fig. 11.

Movie S6: Four modified GRIP control runs, demonstrating how fluctuations in the mean grain size d_g (a, d, g, j) at decimetre
35 scale cause signals to form on the bulk concentration c_B (b, e, h, k); also shown are contemporaneous profiles of the vein radius
 r_v (c, f, i, l). All runs begin at $t = 500$ yr with $c_B \equiv 1 \mu\text{M}$ without an initial impurity signal. Results are shown in the material
reference frame. (a to c) Experiment imposing a negative d_g fluctuation of a fixed width. (d to f) Experiment imposing a
negative d_g fluctuation that has the same initial form as in (a), but which narrows due to vertical compression of the ice. (g to
i) Experiment imposing a positive d_g fluctuation of a fixed width. (j to l) Experiment imposing a positive d_g fluctuation that
40 has the same initial form as in (g), but which narrows under vertical compression. The runs in panels d–f and j–l are stopped
at 40 kyr because, soon afterwards, the d_g fluctuations become too narrow to be resolved by the numerical grid spacing (0.0025
m). In all four runs, the new signal in c_B is localised by the grain-size fluctuation and does not displace into $z' > 0$ by anomalous
diffusion. Snapshots from the movie are reported in Fig. 12.

Movie S7: Four modified EPICA control runs, demonstrating how fluctuations in the mean grain size d_g (a, d, g, j) at decimetre
45 scale cause signals to form on the bulk concentration c_B (b, e, h, k); also shown are contemporaneous profiles of the vein radius
 r_v (c, f, i, l). All runs begin at $t = 4$ kyr with $c_B \equiv 1 \mu\text{M}$ without an initial impurity signal. Results are shown in the material
reference frame. (a to c) Experiment imposing a negative d_g fluctuation of a fixed width. (d to f) Experiment imposing a
negative d_g fluctuation that has the same initial form as in (a), but which narrows due to vertical compression of the ice. (g to
i) Experiment imposing a positive d_g fluctuation of a fixed width. (j to l) Experiment imposing a positive d_g fluctuation that
50 has the same initial form as in (g), but which narrows under compression. In all four runs, the new signal in c_B is localised by
the grain-size fluctuation and does not displace into $z' > 0$ by anomalous diffusion. Snapshots from the movie are reported in
Fig. S3.

Movie S8: Simulations of how a c_B signal in an ice-core sample, stored at (a) -15°C and (b) -5°C , decays as a result of
55 Gibbs–Thomson and residual diffusion. Grey curve depicts the initial signal. The model in Sect. 3.1 (equation (30)) is solved
under the condition of no deformation (i.e. zero vertical strain rate) and zero temperature gradient.

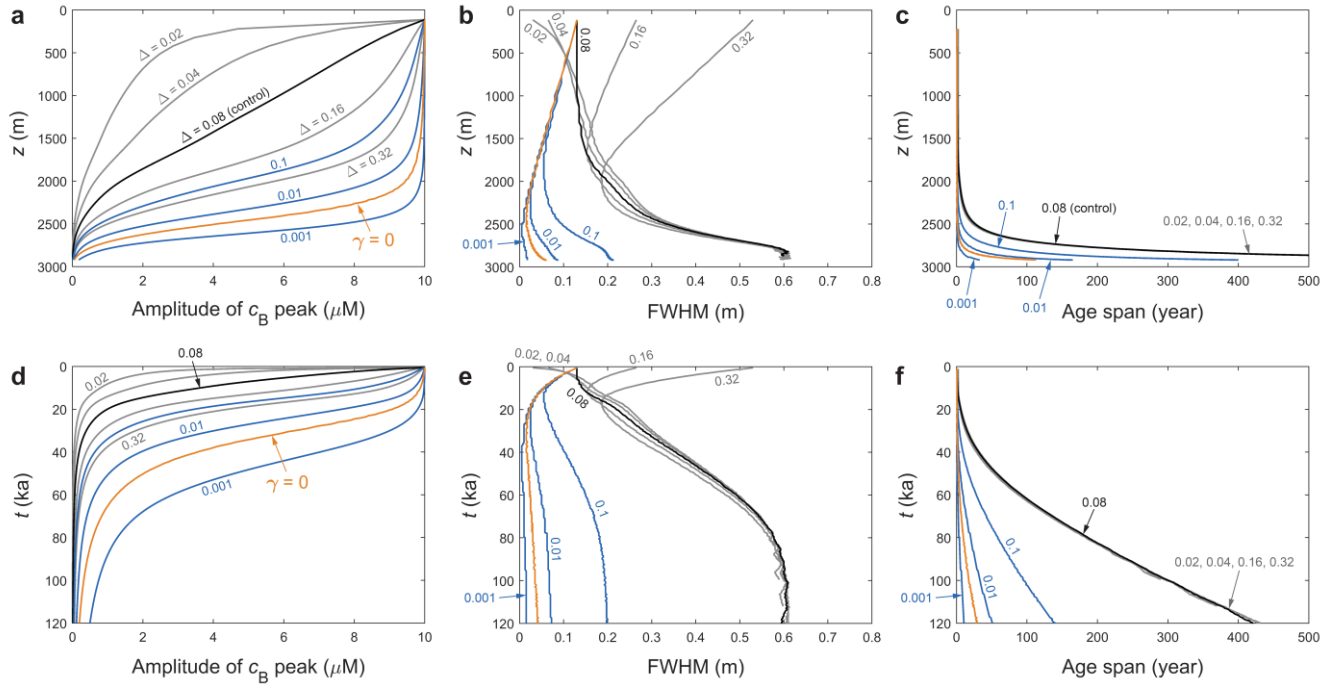


Figure S1: Changing morphometry of the signal peak – its amplitude, full width at half maximum (FWHM), age span – in the
 65 GRIP ice core for different model parameters, plotted against depth (a–c) and age of the ice (d–f). The panel organisation
 follows Fig. 7. The only difference from the experiments in Fig. 7 is that the doped peak here has twice the amplitude, i.e., c_B
 $= 1 + 10\exp[-(z'/\Delta)^2]$. Black curves plot the control run. Orange curves plot the run with the Gibbs-Thomson effect turned off
 ($\gamma = 0$). Grey curves plot the results of altering the width parameter Δ of the doped peak from 0.08 (control) to four other
 values. Blue curves plot the outcomes of suppressing molecular diffusivity D in the control run by the multiplicative factors
 70 0.1, 0.01 and 0.001. Parameter labels use the same colours as the curves.

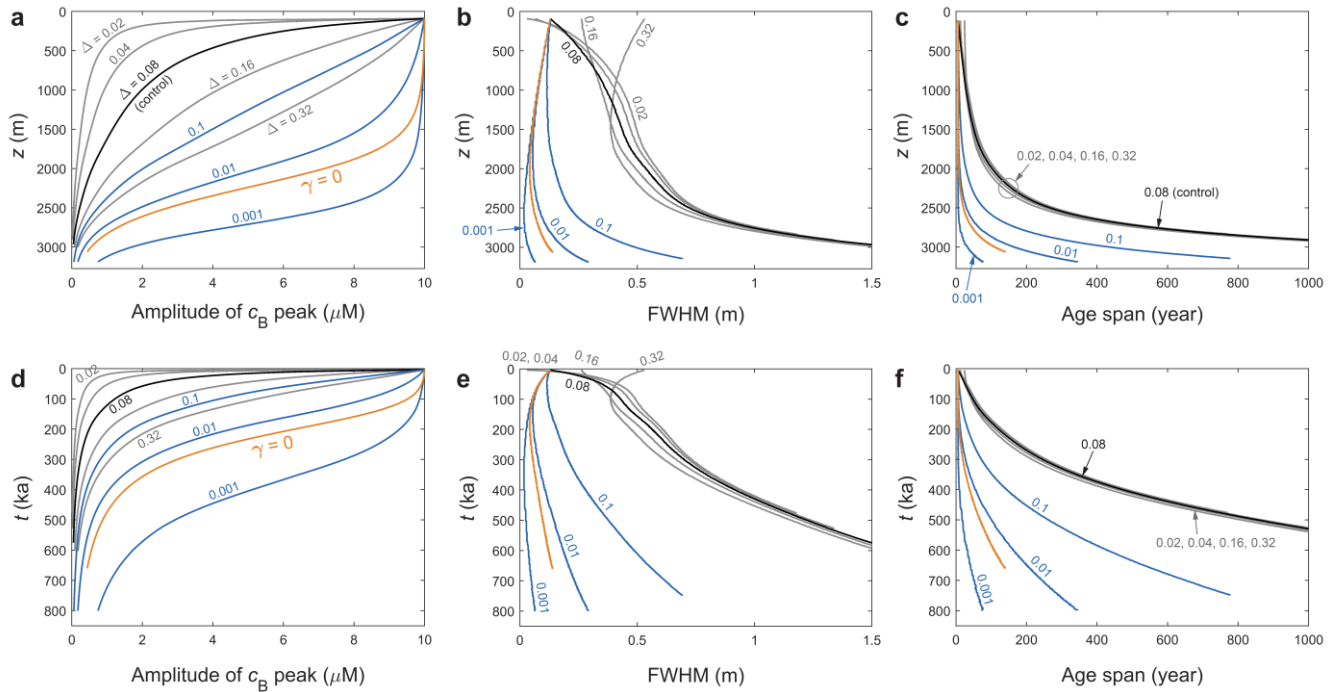
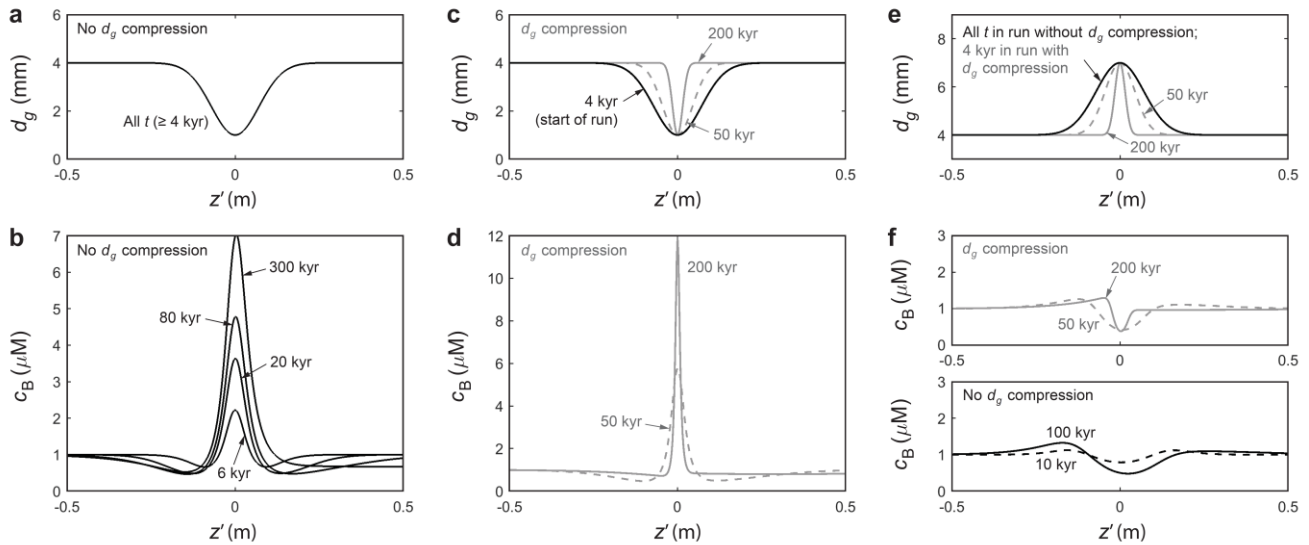


Figure S2: Changing morphometry of the signal peak – its amplitude, full width at half maximum (FWHM), age span – in the EPICA ice core for different model parameters, plotted against depth (a–c) and age of the ice (d–f). The panel organisation follows Fig. 8. The only difference from the experiments in Fig. 8 is that the doped peak here has twice the amplitude, i.e., $c_B = 1 + 10\exp[-(z/\Delta)^2]$. See the caption of Fig. S1 for a guide to the different curves.



95

Figure S3: Four modified EPICA control runs, demonstrating how fluctuations in the mean grain size d_g (a, c, e) at decimetre scale cause signals to form on the bulk concentration c_B (b, d, f). All runs begin at $t = 4$ kyr with $c_B \equiv 1 \mu\text{M}$ without an initial impurity signal. Evolution snapshots are shown in the material reference frame. (a, b) Experiment imposing a negative d_g fluctuation of a fixed width. (c, d) Experiment imposing a negative d_g fluctuation that has the same initial form as in (a), but which narrows due to vertical compression of the ice. (e, f) Two experiments with a positive d_g fluctuation, set up as in the last two experiments. One run assumes that the fluctuation does not experience compression (black curves); the other run assumes that it does (grey). In all four runs, the new signal in c_B is localised by the grain-size fluctuation and does not displace into $z' > 0$ by anomalous diffusion. See Movie S7 for the full simulations.